Fabrication of electrochemical bio-sensors for the detection of glucose and hydrazine using ZnO nanonails grown by the thermal evaporation process

A. Umar, S. H. Kim, J. H. Kim, Y. K. Park and Y. B. Hahn*

School of Chemical Engineering and Technology and Nanomaterials processing Research Centre, Chonbuk National University, Chonju 561-756, South Korea
*Email: ybhahn@chonbuk.ac.kr

ABSTRACT

Well-crystallized zinc oxide nanonails have been synthesized in a large quantity via a thermal evaporation method using the metallic zinc powder without the use of any metal catalyst or additives. The detailed structural and optical characterizations confirmed that the as-synthesized nanonails are single-crystalline with the wurtzite hexagonal phase, grown along the [0001] direction and possessing a good optical properties. For applications point of view, the as-grown ZnO nanonails were used as supporting matrixes for enzyme immobilization, glucose oxidase (GOx), to construct efficient glucose biosensors. The ZnO nanonails have a high surface area and presenting themselves as an efficient electron conducting tunnel, so the GOx attached to the surfaces of ZnO nanonails had more spatial freedom in its orientation, which facilitated the direct electron transfer between the active sites of immobilized GOx and electrode surface. A high sensitivity, 24.613 μA cm^{-2} mM^{-1}, with a response time less than 10s was achieved from the fabricated glucose biosensor. The biosensor shows a linear range from 0.1 to 7.1 mM with a correlation coefficient of R= 0.9937 and the detection limit of 5 μM. Moreover, the detection of hydrazine was performed in a phosphate buffer (pH 6.6). The peak current increases linearly with the concentration of hydrazine from 0.01 to 1mM. This work demonstrates that the ZnO nanostructures can be utilized as an efficient electron mediator to fabricate efficient biosensors.

Keywords: ZnO nanonails; Electrochemical sensors; Glucose sensors; Hydrazine sensors.

1 INTRODUCTION

Among the different electrochemical sensors, electrochemical biosensors hold special positions which are constructed on the amperometric principle based on the oxidation or reductions of electrochemically active substances involved or produce in the reactions. These devices are inherently sensitive and selective towards electroactive species, fast and accurate, compact, portable and inexpensive [1]. Such devices satisfy many of the requirements for on-site environmental analysis. Amperometric enzyme-based biosensors combine enzyme specificity with the sensitivity and convenience of electroanalytical techniques in a compact form to facilitate analysis. Among different types of amperometric biosensors, the amperometric glucose biosensor is important because it is the product of the reactions catalyzed by a large number of oxidases and is of great significance in clinical chemistry and biochemistry [2], environmental monitoring [3] and food chemistry [4]. To increase the selectivity and sensitivity of amperometric glucose biosensors, artificial mediators are often used in the fabrication of biosensors, which are used to transfer electrons between the enzyme and the electrode to allow operation at low potentials [5]. Due to the exotic and versatile properties of the different biocompatible nanomaterials, it was observed that the nanomaterials could be promising mediators for enzyme immobilization, which can increase the sensitivity and selectivity of amperometric biosensors. Therefore, the nanomaterials can keep the activity of enzyme due to desirable microenvironment, and enhance the direct electron transfer between the active sites of enzyme and the electrode. Until now, a number of reports on the fabrication of amperometric glucose sensor based on nanomaterials as an electron mediator are reported in literature. Zhao et al. presented the fabrication of glucose biosensors by modifying the gold electrode using the nanocrystalline diamond [6], Chen et al. have fabricated glucose biosensor using the silicon nanowires prepared by the thermal evaporation process [7], carbon nanotubes nanoelectrode ensembles glucose biosensor has been reported by the Y. Lin et al. [8], Liu et al. reported the horseradish peroxidase amperometric biosensor based on a nanoporous ZrO_2 matrix [9] etc. As a remarkable and functional material II-VI semiconductor, ZnO has attracted extent of scientific and technological attentions. The diversity in the properties of ZnO makes it a versatile material for the wide ranging application possibilities which provide it an opportunity to presents itself as one of the most promising material for the future research and applications. The nanostructures of ZnO are of particular interest as they combine different properties such as high specific surface area, optical transparency, biocompatibity,

non-toxicity, chemical and photochemical stability, ease of fabrication etc. Even having versatile properties, the biosensor applications of ZnO nanostructures are rare.

Here, we present an approach to fabricate effective glucose and hydrazine biosensor using the well-crystallized ZnO nanonails synthesized by the thermal evaporation process. A high sensitivity, 24.613 μA cm^{-2} mM^{-1}, with a response time less than 10s was achieved from the fabricated glucose biosensor. Moreover, the detection of hydrazine was performed in a phosphate buffer (pH 6.6). The peak current increases linearly with the concentration of hydrazine from 0.01 to 1mM.

2 EXPERIMENTAL

The ZnO nanonails were synthesized simply by using the thermal evaporation process as reported previously [10-14]. Typically, a following procedure was employed to synthesize the large-quantity ZnO nanonails: about 2 g of source material, metallic zinc powder was put in a 10 cm long closed end of a slender one-end-sealed quartz tube and placed in the centre of the furnace. Before reaction, the chamber was evacuated to 10^{-1} Torr. The source material was rapidly heated up to the temperature ranges 580-700 °C under a flow of high-purity nitrogen carrier gas at a rate of 200 sccm (standard cubic centimeter per minute). When the furnace temperature reached to the desired growth temperature, the oxygen gas was flowed with a flow rate of 10 sccm during the whole growth period. After the desired time and evaporation process, the white colored product was deposited near the outlet of the quartz tube. These products were scratched and collected from the quartz tube for the examination of their structural and optical properties and for the modification of the electrode surfaces for the effective detection of glucose and hydrazine.

General morphologies of the synthesized ZnO nanonails were observed using the scanning electron microscopy (SEM). The crystallinity and crystal phases of the synthesized structures were investigated by X-ray diffraction (XRD) pattern measured with Cu-Kα radiation. The room- temperature photoluminescence (PL) spectroscopy with the He-Cd (325nm) laser-line as the exciton source was used to examine the optical properties of as-grown ZnO nanonails.

To fabricate the glucose and hydrazine biosensors, the prepared ZnO nanonails were coated to a gold electrode, commonly used in electrochemistry. The prepared ZnO/Gold electrode was then wetted by phosphate buffer solution (PBS) with *p*H = 7.4 in case of glucose detection and PBS solution with *p*H = 6.6, for hydrazine detection and electrodes were dried by high purity nitrogen gas. For the glucose biosensors, the GOx were immobilized onto the ZnO nanonails surfaces. After immobilization with GOx, Nafion solution was dropped onto the modified electrode and dried which form a thin film onto the modified electrode. The electrochemical experiments were performed at room-temperature using an electrochemical analyzer (SHIn 2000, EQCM, Korea) with a conventional three-electrode configuration, a working electrode (ZnO modified gold electrode), a Pt wire as a counter electrode and Ag/AgCl (sat. KCl), as reference electrode. Prior to the experiment, the electrode was polished with aluminum slurries sequentially.

3 RESULTS AND DISCUSSION

3.1 Structural and optical properties of as-grown ZnO nanonails

Figure 1 shows the typical SEM image of the as-grown nanonails and reveals that the nanonails are grown in a very high density. It is attracting to note that the nanonails are arranged in such a special fashion that they are making a perfect spherical open peacock wing like morphologies. Interestingly, it was also observed that the top portion of these structures have a perfectly hexagonal cap which make the nanostructures a nail-like morphology. The diameters of the nanonails bases and tops are in the ranges of 300 ± 50 nm and 70 ± 20 nm, respectively. The caps are about 250 ± 50 nm in diagonal.

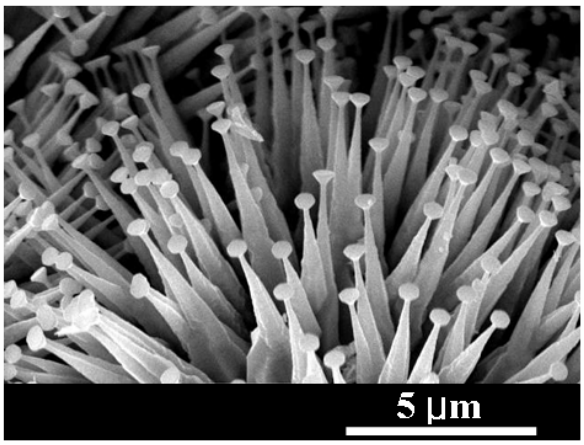

Figure 1: Typical SEM image of the ZnO nanonails grown by thermal evaporation process.

To know the crystallinity and crystal phases of the as-grown ZnO nanonails, XRD studies have been done and shown in Figure 2. All the obtained peaks in the spectrum are well-matched with the typical hexagonal wurtzite ZnO and reveals that the obtained products are the wurtzite hexagonal pure ZnO.

Figure 3 demonstrates the room-temperature PL spectra of the synthesized ZnO nanonails. The appearance of two peaks, a strong, dominated and high intensity peak at 380 nm in the UV region while a suppressed and week band at 521 nm in the visible region, was observed in the spectrum. The UV emission is also called as near band edge emission and originated by the recombination of free-excitons through an exciton-exciton collision process. The green band in the visible region, known as deep level emission, is generally explained by the radial

recombination of the photo-generated hole with the electrons which belongs to the singly ionized oxygen vacancies [10, 11].

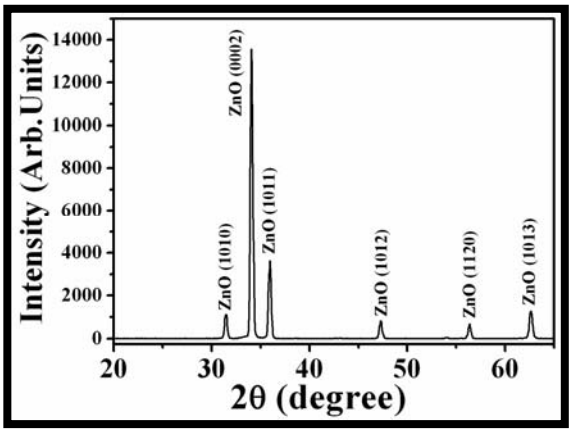

Figure 2: Typical XRD pattern of the grown ZnO nanonails: the indexed peaks are corresponding to the typical wurtzite hexagonal structure for the grown products.

In our case, the UV emission is dominated over the green level emission. It has been reported that the improvement in the crystal quality such as low structural defects, oxygen vacancies, zinc interstitials and decrease in the impurities may cause the appearance of a sharp and strong UV emission and a suppressed and weak green emission [10, 11]. So due to the presence of a strong UV emission and a weak green emission from the synthesized ZnO nanonails indicated that the as-grown structure have good crystal quality with less structural defects.

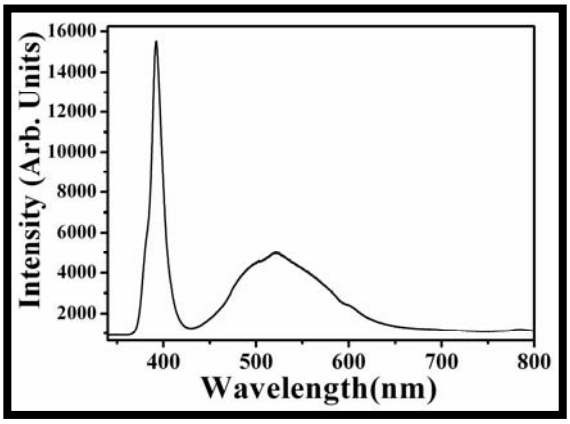

Figure 3: Photoluminescence spectrum of the synthesized ZnO nanonails at room temperature using a He–Cd laser with an excitation wavelength of 325 nm.

3.2 Sensing properties of ZnO nanonails

Figure 4 (a) shows the typical cyclic voltammograms for the Nafion/gold and Nafion/ZnO/gold mentioned as solid and dotted lines, respectively in 0.01M PBS buffer at pH 7.4 at scan rate of 50 mV/s. It was clearly seen from the voltammograms, that two peaks have been appeared from the CV curve of Nafion/ZnO/gold electrodes, which is different from the Nafion/gold electrodes. Due to the good conductivity of ZnO, these peaks are originated by the oxidation and reduction of ZnO itself. ZnO with a high IEP (~9.5) should be suitable for the adsorption of the low IEP enzyme GOx (~4.2). Therefore, the ZnO derived electrodes retained the enzyme bioactivity and could enhance the electron transfer between the enzyme and electrode.

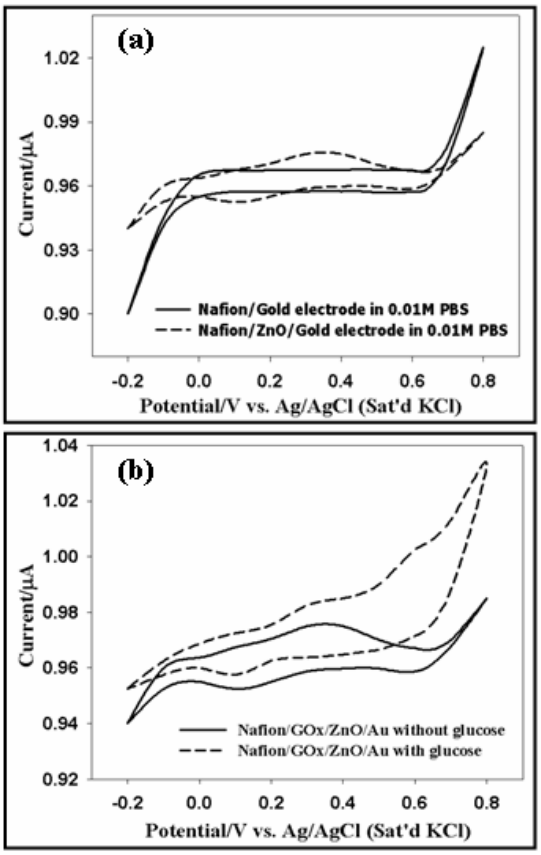

Figure 4: (a) Cyclic voltammograms of Nafion/Au electrode (solid line) and Nafion/ZnO/Au electrode (dotted line) in 0.01 M PBS (pH = 7.4) at scan rate of 50 mV/s. (b) CV curves of the Nafion/GOx/ZnO/Au electrode in the 0.01 M PBS (pH = 7.4) without (solid line) and with (dotted line) of 3 mM glucose.

Figure 4 (b) shows the cyclic voltammograms of Nafion/GOx/ZnO/gold electrode in the same 0.01 M PBS solution in the absence (solid line) and presence (dotted line), respectively of 3 mM glucose. CV curve of Nafion/GOx/ZnO/gold electrode with glucose (dotted line) in PBS shows an increase in current from 0.36 to 0.64 V, as compared to the PBS without glucose, confirming the electrochemical response of the Nafion/GOx/ZnO/gold electrode in glucose. A weak shoulder peak has also been seen from the CV curve of Nafion/GOx/ZnO/gold electrode in PBS with 3mM glucose at 0.58. The origination of this

NSTI-Nanotech 2007, www.nsti.org, ISBN 1420061828 Vol. 1, 2007

shoulder is because of the H_2O_2 generation during the oxidation of glucose by GOx.

Figure 5 shows a cyclic voltammetric sweep curve for a Nafion/ZnO/Gold electrode without (solid line) and with (dotted line) hydrazine in 0.1 M phosphate buffer (pH = 6.6) at the scan rate of 100 mV/s. A well defined oxidation peak is observed from the cyclic voltammograms of the Nafion/ZnO/gold electrode with 1 mM N_2H_4 in 0.1M phosphate buffer with an *E*pa of +0.025V and *I*pa of 0.87 μA. The electrochemical response is irreversible as no cathodic current is observed during the reverse sweep. Hence, the hydrazine has been detected oxidatively at Nafion/ZnO modified gold electrode.

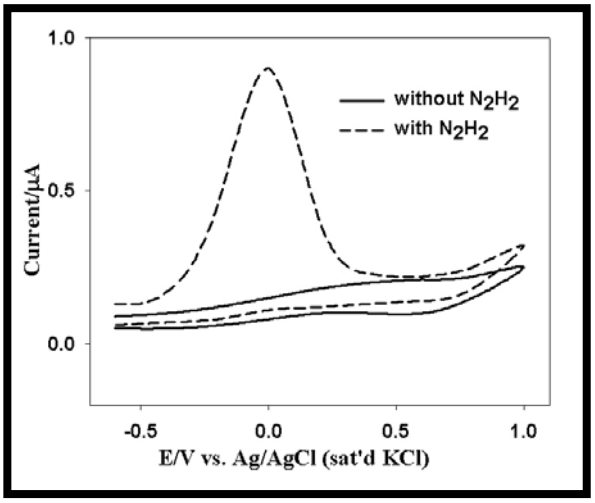

Figure 5: Cyclic voltammograms for a Nafion/ZnO/Gold electrode, without (solid line) and with (dotted line) with 1 mM N_2H_4 in 0.1M phosphate buffer (pH = 6.6). The scan rate was 100 mV/s.

4 CONCLUSION

In conclusion, well-crystallized with good optical properties ZnO nanonails were achieved in a large quantity through a non-catalytic thermal evaporation process. Glucose biosensors were fabricated using the as-grown ZnO nanonails, which act as supporting matrixes for enzyme immobilization, glucose oxidase (GOx). The fabricated ZnO nanonails based glucose biosensors exhibited a high sensitivity, about 24.613 μA cm^{-2} mM^{-1}, with a response time less than 10s and detection limit of 5 μM. Moreover, the detection of hydrazine was performed in a phosphate buffer (pH = 6.6). The peak current increases linearly with the concentration of hydrazine from 0.01 to 1mM. By this work, we can open a new way to utilize ZnO nanostructures as an efficient electron mediator to fabricate efficient sensors.

Acknowledgements:

This work was supported in part by the Brain Korea 21 Project in 2007 and by Korea Research Foundation Grant funded by Korean Government (MOEHRD, KRF-2005-005-J07502).

REFERENCES

[1] S. Park, H. Boo and T. D. Chung, Anal. Chim. Acta 556, 46, 2006.

[2] (a) S.J. Updike, B.J. Gilligan, M.C. Shults and R.K. Rhodes, Diabetes Care 23, 208, 2000, (b) B. Aussedat, V. Thome-Duret, G. Reach, F. Lemmonier, J-C. Klein, Y. Hu and G.S. Wilson, Biosens. Bioelectron. 12, 1061, 1997.

[3] (a) R.W. Keay and C.J. McNeil, Biosens. Bioelectron. 13, 963, 1998; (b) K. Rekha, M.D. Gouda, M.S. Thakur and N.G. Karanth, Biosens. Bioelectron. 15, 499, 2000.

[4] (a) L. Campanella, F. Pacifici, M.P. Sammartino and M. Tomassetti, Bioelectrochem. Bioenerg. 47, 25, 1998; (b) K. Kriz, M. Anderlund and D. Kriz, Biosens. Bioelectron. 16, 363, 2001.

[5] (a) J. Few and H. A. Hill, Anal. Chem. 59, 933A, 1987, (b) N. Morris, M. Cardosi, B. Birch and A. P. Turner, Electroanalysis 4, 1, 1992, (c) (5) M. Green and P. Hilditch, Anal. Proc. 28, 374, 1991.

[6] W. Zhao, J. J. Xu, Q. Q. Qiu and H. Y. Chen, Biosens. Bioelect. 22, 649, 2006.

[7] W. Chen, H. Yao, C. H. Tzang, J. Zhu, M. Yang and S. T. Lee, Appl. Phys. Lett. 88, 213104, 2006.

[8] Y. Lin, F. Lu, Y. Tu and Z. Ren, Nano Lett. 4, 191, 2004.

[9] B. H. Liu, Y. Cao, D. D. Chen, J. L. Kong and J. Q. Deng, Anal. Chim. Acta 478, 59, 2003.

[10] A. Umar and Y. B. Hahn, Appl. Phys. Lett. 88, 173120, 2006.

[11] A. Umar and Y. B. Hahn, Nanotechnology 17, 2174, 2006.

[12] A. Umar, B Karunagaran, E-K Suh and Y B Hahn, Nanotechnology 17, 4072, 2006.

[13] A. Umar, S.H. Kim, Y. S. Lee, K. S. Nahm and Y. B. Hahn, J. Cryst. Growth 282, 131, 2005.

[14] A. Umar, E. K. Suh and Y. B. Hahn, Solid State Commun. 139, 447, 2006.